Sixth International Symposium on Turbulence and Shear Flow Phenomena
Seoul, Korea, 22-24 June 2009

REYNOLDS STRESS TRANSPORT MODELS IN UNSTEADY AND NON-EQUILIBRIUM TURBULENT FLOWS

Sharaf F. Al-Sharif*, Mark A. Cotton & Tim J. Craft
School of Mechanical Aerospace, and Civil Engineering,
The University of Manchester
PO Box 88, Manchester M60 1QD, UK
*sharaf.f.al-sharif@postgrad.manchester.ac.uk

ABSTRACT

In this work the predictive capability of a number of Reynolds stress transport (RST) models was first tested in a range of non-equilibrium homogeneous flows, comparisons being drawn with existing direct numerical simulation (DNS) results and physical measurements. The cases considered include both shear and normally strained flows, in some cases with a constant applied strain rate, and in others where this varied with time. Subsequently, the models were also tested in the inhomogeneous case of pulsating channel flow over a wide range of frequencies.

Models were generally found to perform well in homogeneous shear at low shear rates, but their performance increasingly deteriorated at higher shear rates. This was attributed mainly to over-predicted shear stress anisotropy at high shear rates. Performance in irrotational homogeneous strains was generally good, and was more consistent over a much wider range of strain rates.

In the pulsating channel flows, the most challenging case for the models was found to be the lowest frequency case where, because of the amplitude of oscillation, laminarization and re-transition to turbulence were present at certain phases of the cycle.

INTRODUCTION

The need for reliable and accurate simulations of unsteady, non-equilibrium turbulent flows arises in many fields of engineering and scientific studies. Examples include internal combustion engines, aerofoils at high angles of incidence, coastal hydrodynamics, and the flow of blood in veins and arteries, to name but a few. The requirements of unsteady or largely off-design simulations stretch, and are sometimes beyond, the capabilities of standard eddy-viscosity based Reynolds-averaged treatments of turbulent flows. Nevertheless, typical time and cost limitations make it highly desirable to be able to tackle such problems with an averaged approach that is sensitive to the non-equilibrium effects on the flow quantities of interest, while avoiding the need for high-resolution approaches. Reynolds stress transport (RST) models potentially offer some of this desired sensitivity to unsteadiness and non-equilibrium conditions by allowing for misalignment between mean velocity gradients and turbulent stresses that can affect the rate of production of turbulence. However, other important aspects of flow non-equilibrium, such as delays in the transfer of energy across the turbulence spectrum, are not built-in. Moreover, it is not clear *a priori* how the principal modelled elements in the stress transport equations, particularly pressure-strain rate redistribution, are themselves affected by non-equilibrium conditions. It is thus desirable to test existing models in a wide range of unsteady non-equilibrium flows to identify the major strengths and weaknesses of the models and main areas requiring improvement.

The present work thus aims to study the performance of a number of existing Reynolds stress transport models in a range of non-equilibrium flows. The models tested include the LRRIP model of Launder et al. (1975) (the 'Basic Model'), the SSG model of Speziale et al. (1991), the Shima (1998) Low-Re model, and the TCL model (Craft, 1998; Craft and Launder, 2002). Both homogeneous and inhomogeneous flows have been considered. Here, results are first reported for homogeneous shear flows, both with constant shear rates and also for a case with a time-varying shear. Some irrotational, plane-strain, cases are then presented, again with both constant and time-varying strain rates. Finally, applications are reported to pulsed channel flows over a range of forcing frequencies. None of the models tested reproduce all the flows correctly, and the sections below attempt to highlight the relative strengths and weaknesses of the schemes.

TURBULENCE MODELS

The Reynolds stress transport equation can be written in short form as

$$\frac{\mathrm{D}\overline{u_i u_j}}{\mathrm{D}t} = P_{ij} + \phi_{ij} + T_{ij} + V_{ij} - \varepsilon_{ij} \tag{1}$$

where the the right hand side terms represent production, pressure-strain rate redistribution, turbulent diffusion, viscous diffusion, and dissipation of Reynolds stress, respectively. Production is given exactly in closed form by

$$P_{ij} = -\overline{u_i u_k}\frac{\partial U_j}{\partial x_k} - \overline{u_j u_k}\frac{\partial Ui}{\partial x_k} \tag{2}$$

Similarly, viscous diffusion is given exactly by

$$V_{ij} = \nu\frac{\partial^2(\overline{u_i u_j})}{\partial x_k \partial x_k} \tag{3}$$

The dissipation rate tensor is most often assumed to be isotropic

$$\varepsilon_{ij} = \frac{2}{3}\varepsilon\delta_{ij} \tag{4}$$

where ε is the scalar rate of dissipation of turbulent kinetic energy and is obtained from a modelled transport equation

$$\frac{\mathrm{D}\varepsilon}{\mathrm{D}t} = C_{\varepsilon 1}\frac{\varepsilon}{k}P_\kappa - C_{\varepsilon 2}\frac{\varepsilon^2}{k} + \frac{\partial}{\partial x_k}\left(C_\varepsilon \frac{k}{\varepsilon}\overline{u_k u_l}\frac{\partial \varepsilon}{\partial x_l} + \nu\frac{\partial \varepsilon}{\partial x_k}\right) \tag{5}$$

where $P_\kappa = P_{kk}/2$ and the standard values of the coefficients are $C_{\varepsilon 1} = 1.44$, $C_{\varepsilon 2} = 1.92$, and $C_\varepsilon = 0.15$.

The most widely used model for the turbulent diffusion is the generalized gradient diffusion hypothesis (GGDH) of

Daly and Harlow (1970)

$$T_{ij} = \frac{\partial}{\partial x_l}\left(C_s \frac{k}{\varepsilon}\overline{u_l u_k}\frac{\partial \overline{u_i u_j}}{\partial x_k}\right) \tag{6}$$

where $C_s = 0.22$.

The 'Basic Model'

The pressure strain rate term ϕ_{ij} is comprised of a non-linear turbulence-turbulence interaction or 'slow' term ϕ^s_{ij}, a 'rapid' term that arises from interaction with the mean velocity gradient, ϕ^r_{ij}, and corresponding terms that arise from interaction of the previous terms with walls, thus

$$\phi_{ij} = \phi^s_{ij} + \phi^r_{ij} + \phi^{w,s}_{ij} + \phi^{w,r}_{ij} \tag{7}$$

In homogeneous turbulence, the last two terms are zero. The basic RST model uses Rotta's Return-to-Isotropy model for the slow pressure strain rate term:

$$\phi^s_{ij} = -C_1 \varepsilon a_{ij} \tag{8}$$

and the Isotropization of Production (IP) model for the rapid term,

$$\phi^r_{ij} = -C_2(P_{ij} - \tfrac{2}{3}P_\kappa\,\delta_{ij}) \tag{9}$$

The wall interaction terms in the basic model employ 'wall reflection' terms that are based on wall-normal vectors and distances to walls.

For turbulent diffusion the generalized gradient diffusion model of equation (6) is used.

The Shima Low-Re model

In its original form the Launder and Shima (1989) model is a low-Re version of the Basic Model that uses wall reflection terms and includes damping coefficients to return the correct near-wall behaviour. Later Shima (1998) developed an alternative model, based on the Quasi-Isotropic (QI) model of ϕ^r_{ij} described in Launder et al. (1975), that discards the use of wall-reflection terms that depend on wall-normal vectors and distances, with the aim of improving the applicability and generality of the models. In this version

$$\begin{aligned}\phi^r_{ij} = &-C_2(P_{ij} - 2/3P_\kappa\delta_{ij}) - C_3(D_{ij} - 2/3D_\kappa\delta_{ij}) \\ &- C_4 k\left(\frac{\partial U_i}{\partial x_j} + \frac{\partial U_j}{\partial x_i}\right)\end{aligned} \tag{10}$$

where

$$D_{ij} = -\overline{u_i u_k}\frac{\partial U_k}{\partial x_j} - \overline{u_j u_k}\frac{\partial Uk}{\partial x_i} \tag{11}$$

$D_\kappa = D_{kk}/2$ and the coefficients are given by

$$\begin{aligned}C_1 &= 1 + 2.45A_2^{0.25}A^{0.75}[1-\exp(-49A^2)] \\ &\quad\times\{1-\exp[-(Re_t/60)^2]\} \\ C_2 &= 0.7A \\ C_3 &= 0.3A^{0.5} \\ C_4 &= 0.65A(0.23C_1 + C_2 - 1) + 1.3A_2^{0.25}C_3\end{aligned} \tag{12}$$

where $A = 1 - 9/8(A_2 - A_3)$ is the 'flatness' parameter, and $A_2 = a_{ij}a_{ji}$, $A_3 = a_{ij}a_{jk}a_{ki}$ are the second and third invariants of the stress anisotropy tensor respectively.

The TCL Model

The TCL model (Craft, 1998; Craft and Launder, 2002) was developed based on the principle of maintaining realizability in the limit of two component turbulence, when one of the normal stress components drops to zero, as occurs near a wall or free surface. In this model the slow pressure-strain rate term is given by

$$\phi^s_{ij} = -C_1\varepsilon[a_{ij} + C_1'(a_{ik}a_{kj} - \tfrac{1}{3}A_2\delta_{ij})] - f'_A\varepsilon a_{ij}\,, \tag{13}$$

where the coefficients are given by

$$\begin{aligned}C_1 &= 3.1(AA_2)^{1/2} \\ C_1' &= 1.1 \\ f'_A &= \sqrt{A}f_{\mathrm{Re_t}} + A(1-f_{\mathrm{Re_t}}) \\ f_{\mathrm{Re_t}} &= \min[(\mathrm{Re_t}/160)^2, 1]\end{aligned} \tag{14}$$

The rapid pressure-strain rate term is given by

$$\begin{aligned}\phi^r_{ij} = &-0.6\,(P_{ij} - 2/3\delta_{ij}P) + 0.6a_{ij}P \\ &- 0.2\Bigg\{\frac{\overline{u_k u_j}\,\overline{u_l u_i}}{k}\left[\frac{\partial U_k}{\partial x_l} + \frac{\partial U_l}{\partial x_k}\right] \\ &\quad - \frac{\overline{u_l u_k}}{k}\left[\overline{u_i u_k}\frac{\partial U_j}{\partial x_l} + \overline{u_j u_k}\frac{\partial U_i}{\partial x_l}\right]\Bigg\} \\ &- c_2\Big\{A_2(P_{ij} - D_{ij}) + 3a_{mi}a_{nj}(P_{mn} - D_{mn})\Big\} \\ &+ c_2'\Bigg\{\left(\frac{7}{15} - \frac{A_2}{4}\right)(P_{ij} - 2/3\delta_{ij}P) \\ &+ 0.2[a_{ij} - 1/2(a_{ik}a_{kj} - 1/3\delta_{ij}A_2]P - 0.05a_{ij}a_{lk}P_{kl} \\ &+ 0.1\left[\frac{\overline{u_i u_m}}{k}P_{mj} + \frac{\overline{u_j u_m}}{k}P_{mi} - 2/3\,\delta_{ij}\frac{\overline{u_l u_m}}{k}P_{ml}\right] \\ &+ 0.1\left[\frac{\overline{u_l u_i}\,\overline{u_k u_j}}{k^2} - 1/3\,\delta_{ij}\frac{\overline{u_l u_m}\,\overline{u_k u_m}}{k^2}\right] \\ &\quad\times\left[6D_{lk} + 13k\left(\frac{\partial U_l}{\partial x_k} + \frac{\partial U_k}{\partial x_l}\right)\right] \\ &+ 0.2\frac{\overline{u_l u_i}\,\overline{u_k u_j}}{k^2}(D_{lk} - P_{lk})\Bigg\}\end{aligned} \tag{15}$$

In its earliest High-Re formulation, the TCL model used constant coefficients $C_2 = 0.55$, $C_2' = 0.6$. This was later abandoned in Low-Re versions of the model to allow for near wall corrections. The coefficients used here, in the later versions are given as

$$\begin{aligned}C_2 &= \min\left\{0.55\left[1 - \exp\left(\frac{-A^{1.5}\mathrm{Re_t}}{100}\right)\right]\,,\ \frac{3.2A}{1+S^*}\right\} \\ C_2' &= \min(0.6, A) + \frac{3.5(S^* - \Omega^*)}{3 + S^* + \Omega^*} - 2\min[S_I, 0]\end{aligned} \tag{16}$$

However, as will be seen below, the original prescription with constant coefficients was found to have some merits in homogeneous shear flows.

An *anisotropic* dissipation tensor is used in this model, and is given by

$$\varepsilon_{ij} = (1-f_\varepsilon)\frac{\varepsilon'_{ij} + \varepsilon''_{ij} + \varepsilon'''_{ij}}{D} + \tfrac{2}{3}f_\varepsilon\varepsilon\delta_{ij} \tag{17}$$

In homogeneous turbulence this reduces to

$$\varepsilon_{ij} = (1-f_\varepsilon)\,\varepsilon\frac{\overline{u_i u_j}}{k} + \tfrac{2}{3}f_\varepsilon\varepsilon\delta_{ij} \tag{18}$$

where $f_\varepsilon = A^{3/2}$. Due to space limitation, the remaining elements of (17), and other elements pertaining to the inhomogeneous parts of ϕ_{ij} and diffusion terms will not be listed here. Interested readers are referred to Craft (1998).

HOMOGENEOUS TURBULENCE

Homogeneous turbulence is a special case in which all spatial gradients of turbulent statistics are negligibly small. For this to hold, the mean velocity gradients, if present, are allowed to vary in time but not in space. While this severe restriction means such flows are of little practical interest, the great simplification of the governing equations that results, and the fact that the turbulence is effectively decoupled from the mean flow, makes homogeneous turbulence very attractive from a theoretical view point, particularly as a means for model testing and development.

Turbulence kinetic energy in this case is governed by the exact equation

$$\frac{\mathrm{D}k}{\mathrm{D}t} = P_\kappa - \varepsilon \tag{19}$$

Homogeneous Turbulent Shear

The first set of test cases pertains to homogeneous turbulent shear flow where the mean velocity gradient is constant and the only non-zero component is given by $\frac{\partial U}{\partial y} = S$.

The initial shear parameter $S_0^* = \frac{Sk_0}{\varepsilon_0}$ varied in the range from 1 to 50. Evolution of the turbulent kinetic energy and the a_{11}, a_{12} components of Reynolds stress anisotropy for three values of the initial shear parameter is shown in Figure 1. Model predictions are compared to DNS results of Rogers and Moin (1987) for the case $S_0^* = 1.2$, Matsumoto et al. (1991) for $S_0^* = 4.7$, and Lee et al. (1990) for $S_0^* = 16.75$. At the lowest initial shear rate, both k and the stress anisotropy are reasonably well predicted by all the models. This was generally found to be true in cases where the initial shear parameter is less than 4. At the intermediate shear rate $S_0^* = 4.7$, the Basic and TCL models over-predict the rate of growth of k. This is due to the slight over-prediction of the a_{12} magnitude by these models. The

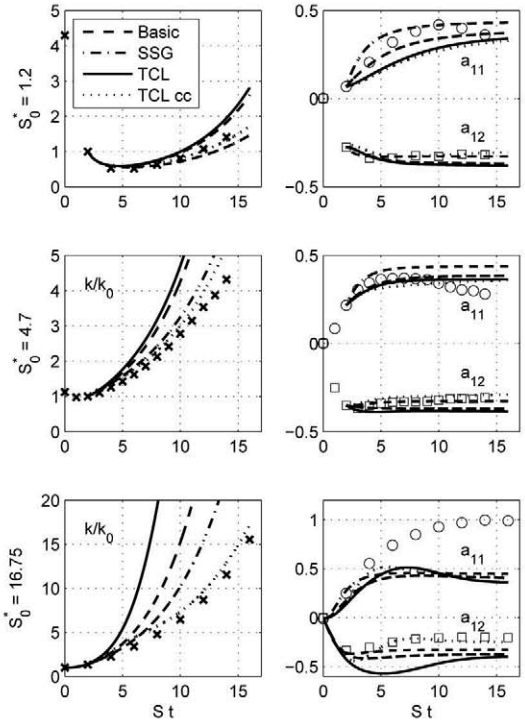

Figure 1: Evolution of turbulent kinetic energy (left) and a_{11},a_{12} components of anisotropy (right) in simple homogeneous shear at various shear rates.

SSG model, and the TCL model using constant C_2 and C_2' coefficients (labelled TCL cc) do not suffer from this over-prediction, and thus more accurately reproduce the growth of k. It can be said that at this level of shear the anisotropy is still qualitatively correct.

At the highest shear rate of $S_0^* = 16.75$ there is a marked qualitative change in the behaviour exhibited by the turbulence statistics. Due to the high shear rate in this case, the DNS results resemble the Rapid Distortion Theory (RDT) solution for simple shear, as confirmed by Lee et al. (1990). In the limit of rapid distortion, simply-sheared homogeneous turbulence tends towards a one-component limit, where all of the energy is contained in the $\overline{u^2}$ component, the $\overline{uv}$ component is suppressed, and the asymptotic growth of k is linear rather than exponential (Pope, 2000). These trends are seen in the bottom row of Figure 1; specifically, the normal anisotropy a_{11} is markedly higher than in the previous cases, and is largely under-predicted by the models, and the magnitude of the turbulence energy-producing a_{12} is lower than in previous cases, and over-predicted by almost all the models. The over-prediction of a_{12} leads to an exaggerated rate of growth of k. The notable exception to this is the TCL model using constant coefficients C_2, C_2'. The currently used variable prescription of these coefficients was found by Craft (1998) to improve the model's performance in the backward facing step problem, where it was noted that higher C_2 contributed an excessively large sink for the shear stress (Craft, 1998). It is precisely this behaviour that is desired in this problem where, as the RDT solution predicts, a_{12} decays.

Oscillating Homogeneous Shear

The next set of cases was that of turbulent flow subjected to an oscillating shear rate given by

$$\frac{\partial U}{\partial y} = S(t) = S_{\max}\sin(\omega t) \tag{20}$$

The reference data for this set of cases is the DNS of Yu and Girimaji (2006), who carried out simulations for the range of frequencies $0.125 < \omega/S_{\max} < 10$.

The DNS and modelled evolution of k/k_0 at different forcing frequencies (up to $\omega/S_{\max} = 1.0$) are shown in Figure 2. It can be seen that turbulence energy grows (on average) at the lower frequencies of the applied shear, and decays at high frequencies. Yu and Girimaji identified the frequency at which this change in behaviour occurs to be around $\omega/S_{max} \sim 0.5$. The critical mechanism determining whether k grows or decays is the phase shift between the shear stress $\overline{uv}$ and the applied rate of shear $\frac{\partial U}{\partial y}$. The models correctly reproduce this qualitative change of behaviour between low and high frequencies, due to the intrinsic quality of RST models, where the Reynolds stresses are obtained from individual transport equations, and thus need not be in phase with the mean strains. The observed critical frequency at which the growth behaviour changes appears to be picked up most closely by both versions of the TCL model. The TCL model with constant C_2 and C_2' coefficients returns the best results over the whole range considered, while the version with variable coefficients significantly over-predicts the rate of growth of k at the lower frequencies.

Irrotational Strain Rates

Another class of homogeneous turbulence test cases considered is that of irrotational mean strain rates. These include plane strain and axisymmetric contraction and ex-

pansion. Due to space limitation, only the plane strain results are presented here.

In plane strain the production of turbulent kinetic energy is given by $P_\kappa = S_{11}k(a_{22} - a_{11})$. The strain parameter for this case is defined as $S^* = S_{11}k/\varepsilon$. The reference data set for this case is the DNS of Lee and Reynolds (1985). Turbulent kinetic energy and stress anisotropy evolution under plane strain is shown in Figure 3 for three initial strain parameters, $S_0^* = 0.5, 4, 77$. One immediately notices that, in contrast to homogeneous shear, the k evolution is quite well predicted over a much larger range of S^*. This is true even for the models whose anisotropy evolution tends to deviate from the reference data. Evidently, both a_{22} and a_{11} appear to deviate in the same direction, and since it is the difference $a_{22} - a_{11}$ that determines P_κ, the errors tend to cancel and the kinetic energy evolution is well predicted. Unfortunately, due to the short integration time of the reference data, one cannot know how well this holds over longer periods.

The stress anisotropy evolution is remarkably well reproduced by the TCL model with variable coefficients over the whole range of strain rates, while the opposite is true for the version using constant coefficients. This is in sharp contrast to the homogeneous shear cases, both constant and time-varying, where the version with constant coefficients gave the better results. This suggests a significantly different behaviour of the pressure-strain rate redistribution in rotational and irrotational strains, highlighting the conflicting requirements on model coefficients.

Another irrotational strain case studied here is the successive plane strain-relaxation-destraining experiment of Chen et al. (2006). The form of the mean velocity gradient is the same as in the preceding set of cases, but the strain rate S_{11} now varies in time. This time-varying applied strain rate is shown in the top plot of Figure 4, and the Reynolds stress components $\overline{u^2}, \overline{v^2}$ (labelled as R_{11} and R_{22}) are shown in the the bottom plot normalised by their initial values. All the models return the correct $\overline{v^2}$ evolution up to the point at which $S_{11}(t)$ peaks, after which they all over-predict this stress component, with the TCL giving the least over-prediction. The magnitude of $\overline{u^2}$ is under-predicted throughout the cycle, but to a lesser extent. Unfortunately, since the third stress component was not measured in the experiment, it is not possible to tell to what extent these over-predictions are the result of an over-predicted level of turbulence energy, or degree of anisotropy. If one assumes that the redistribution is adequately accounted for, at least by the TCL as in the previous plane strain cases, the rapid decay of $\overline{v^2}$ after the peak of straining suggests an accelerated turbulence dissipation rate.

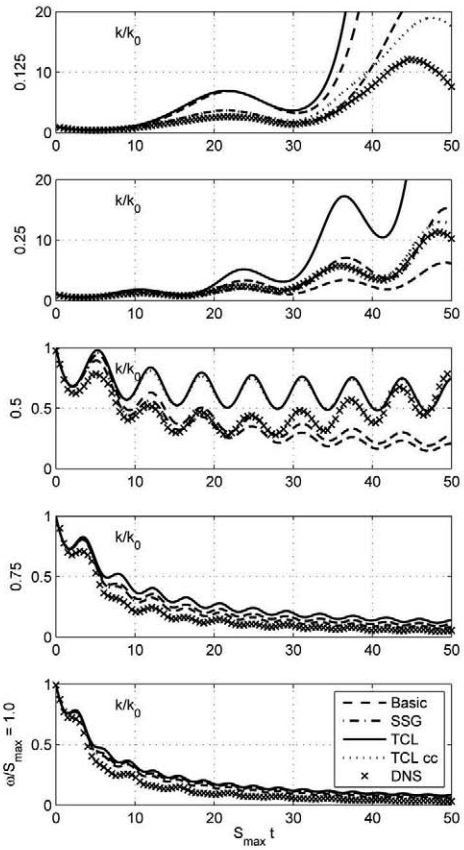

Figure 2: Evolution of k/k_0 in oscillating homogeneous shear.

PULSATING CHANNEL FLOWS

A range of oscillating internal (pipe and channel) flows has also been examined. Briefly presented here is a set of cases pertaining to pulsating channel flow driven by an oscillating pressure gradient at three non-dimensional frequencies of $\omega^+ = 0.0016$, 0.01, 0.04, where $\omega^+ = \omega\nu/\overline{u_\tau}$ and $\overline{u_\tau}$ is the time-averaged wall friction velocity. The reference for this case is the LES of Scotti and Piomelli (2001). The amplitude of pressure oscillations was varied dramatically in order to maintain a fairly constant amplitude of centre-line velocity oscillations, around 70%, so that flow reversal was observed in the near wall region. This set of cases has proven to be quite challenging for the models. This is particularly true for the low frequency case, where the flow was found to experience cyclic laminarization and transition back to turbulence.

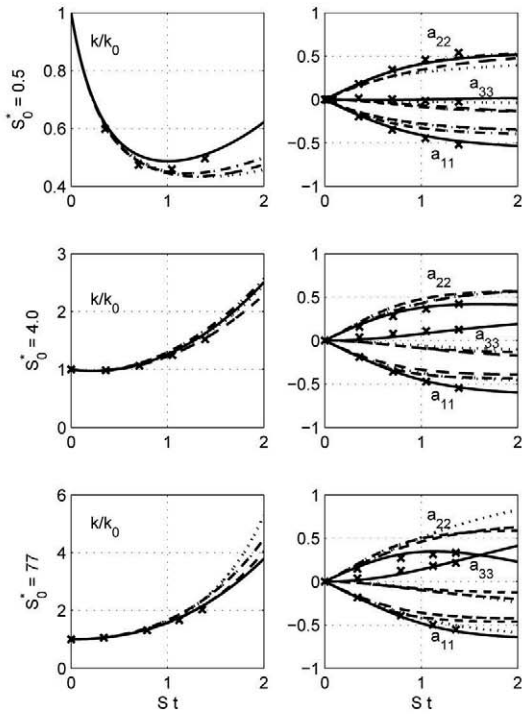

Figure 3: Evolution of turbulent kinetic energy (left) and Reynolds stress anisotropy (right) in plane strain at various strain rates.

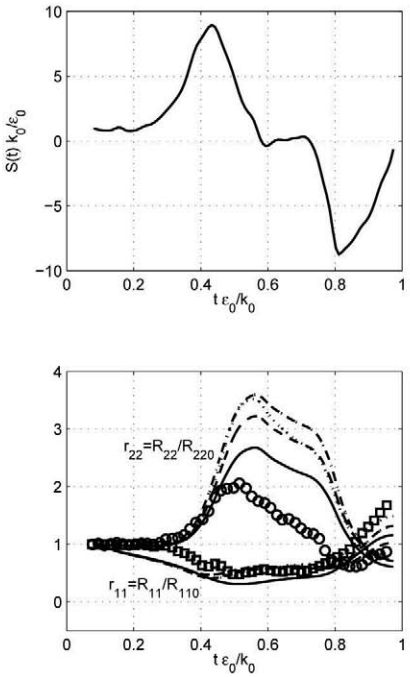

Figure 4: Successive plane straining-destraining experiment of Chen et al. (2006). Top: applied strain rate. Bottom: $\overline{u^2}, \overline{v^2}$ Reynolds stresses normalised by their initial value.

In the Scotti and Piomelli (2001) simulations, turbulent channel flow is subjected to an applied pressure gradient given by

$$\left\langle \frac{\mathrm{d}p}{\mathrm{d}x} \right\rangle = \overline{\frac{\mathrm{d}p}{\mathrm{d}x}} + \left| \frac{\mathrm{d}p}{\mathrm{d}x} \right| \cos(\omega t) \tag{21}$$

The phase-averaged velocity is governed by

$$\frac{\partial U}{\partial t} = -\frac{1}{\rho}\frac{\mathrm{d}p}{\mathrm{d}x} + \frac{\partial}{\partial y}\left(\nu \frac{\partial U}{\partial y} - \overline{uv}\right) \tag{22}$$

The Reynolds number based on mean friction velocity u_τ is $Re_\tau = 350$. The flow exhibits two limiting behaviours depending on the frequency. At the limit of very low frequencies, when the rate of variation of mean flow quantities is very small, the turbulence has ample time to adjust to the changing flow conditions. The flow in this limit behaves as if progressing through a series of equilibrium states at different conditions, hence it is called the quasi-steady limit. At the other extreme, when the frequency is sufficiently high the inertia of the bulk flow confines fluctuations of flow quantities to a small region near the wall, and the turbulence is 'frozen' in the outer region. At the point when fluctuations are confined to the viscosity affected region, the flow mimics the laminar solution of this problem, and this is hence called the quasi-laminar limit. The examined frequencies of $\omega^+ = 0.0016$, 0.01, 0.04 correspond roughly to the low, intermediate and high frequency regimes, respectively.

Some sample results are presented in Figures 5 and 6 showing profiles of phase-averaged velocity and turbulent kinetic energy, respectively, for the high frequency case $\omega^+ = 0.04$. Results were obtained using the Shima and TCL models, and the low-Re k-ϵ model of Launder and Sharma (1974) has also been used for comparison. At this frequency, the Shima model tends to under-predict the velocity throughout the cycle, while the TCL model agrees best with the LES data in this respect. In Figure 6 it can be seen that because of the high frequency in this case, cyclic variations in k are concentrated in the near-wall region where none of the models is able to fully reproduce the peak in the k profile, which is consistently under-predicted in this region. In the outer region k is seen to remain at a fairly constant level, as expected at high frequency, and all of the models give broadly the right shape of profile for k in this region. An alternative view of the data is provided in Figure 7 showing cyclic variations of flow quantities at a fixed location of $y^+ = 18$, and Figure 8 shows similar graphs for the lowest frequency case $\omega^+ = 0.0016$ at $y^+ = 19$. This latter figure reveals some of the difficulty that the models face by laminarization and re-transition within the cycle, where the flow variables are seen to undergo an abrupt change in the re-transition phase. This is more pronounced in the TCL model, as evidenced by the 'kink' in the graphs. This is most likely due to the damping coefficients in the models which are designed to return the correct near-wall behaviour in steady flow. In this periodic case the flow quantities, in particular $\mathrm{Re_t} = k^2/\nu\varepsilon$, cyclically oscillate about the values used in the coefficient 'switches' that were appropriate in steady flow, thus producing abrupt variations in the coefficients that adversely affect the profiles of the variables. The Shima model did not recover from the laminarization phase of the cyle in this case, and it was not possible to obtain a periodic turbulent solution using it.

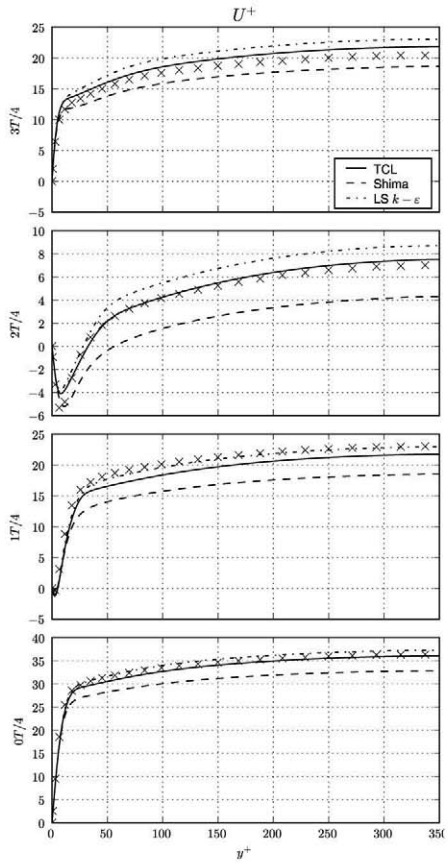

Figure 5: Profiles of phase-averaged velocity at $\omega^+ = 0.04$. Symbols represent data of Scotti and Piomelli (2001).

CONCLUSIONS

In simple shear it was generally found that models predict the correct evolution of turbulent kinetic energy k and dissipation rate ε at lower dimensionless shear rates $Sk/\varepsilon < 4$. There is some variation among the models in the quality of the anisotropy prediction, but the more impor-

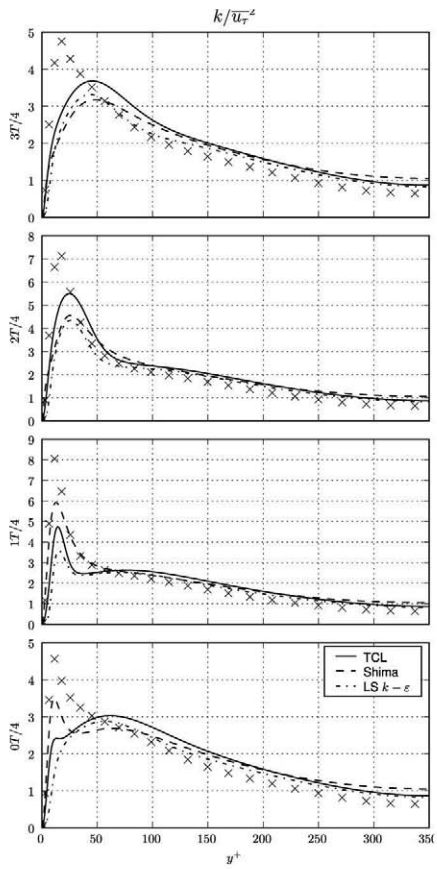

Figure 6: Profiles of turbulent kinetic energy at $\omega^+ = 0.04$

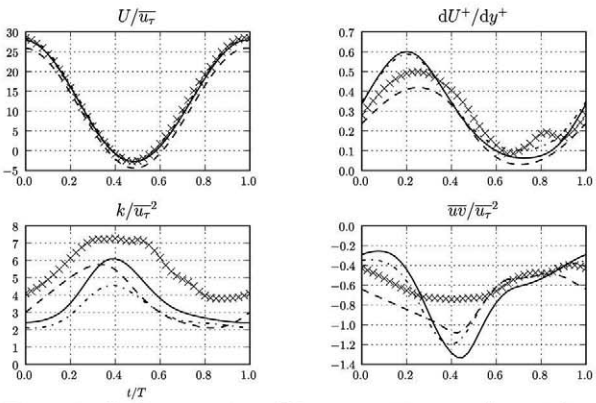

Figure 7: Cyclic variation of flow quantities at $y^+ = 18$ for the high frequency case $\omega^+ = 0.04$. Key as in Figure 6.

tant components a_{12}, a_{11} are reasonably well predicted by most models. At the higher shear rates tested, $Sk/\varepsilon > 16$, existing models grossly over-predict the evolution of k and ε. This is attributed mainly to the inability of the models to replicate the decay of a_{12} at high shear rates as predicted by Rapid Distortion Theory (RDT), and observed in DNS results. In addition, the normal stress anisotropies are also under-predicted by the models. It is observed that with some modifications to the coefficients of the pressure-strain rate correlation, it is possible to correct the former at least, thus correcting the rate of evolution of k and ε.

In the case of homogeneous turbulence subjected to oscillating shear the models generally returned the correct qualitative trend of turbulence energy growth at low frequencies and decay at high frequencies. The critical frequency at which this change in behaviour occurs depends on the modulation of the shear stress and the applied shear, and is picked up most closely by the TCL model.

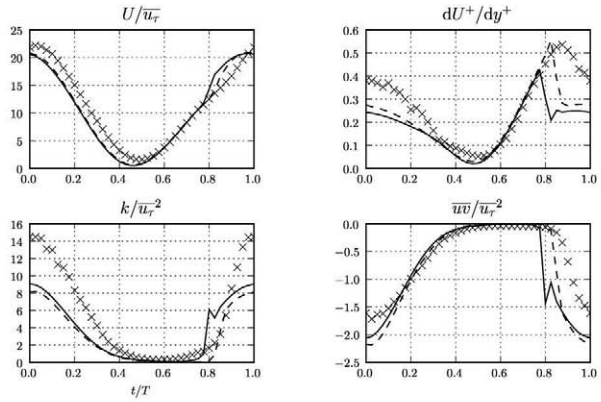

Figure 8: Cyclic variation of various flow quantities at $y^+ = 19$ for the high frequency case $\omega^+ = 0.0016$. Solid line: TCL; dashed line: LS.

Model performance was found to be consistent over a much wider range of strain rates in the homogeneous irrotational strain cases, where the Low-Re TCL model was found to return the best results.

In pulsating channel flow, the models performed reasonably well in the high frequency case, where the flow approached the quasi-laminar behaviour. The lowest frequency case was found to be the most challenging due to cyclic laminarization and re-transition. This suggests a need for reformulating the near-wall damping in some of the model coefficients to allow them to handle this cyclic transition more gracefully.

REFERENCES

Chen, J., Meneveau, C., and Katz, J.: 2006, *J. Fluid Mech.* **562**, 123

Craft, T.: 1998, *Int. J. Heat and Fluid Flow* **19**, 541

Craft, T. and Launder, B.: 2002, in B. Launder and N. Sandham (eds.), *Closure Strategies for Turbulent and Transitional Flows*, Cambridge University Press

Daly, B. and Harlow, F.: 1970, *Phys. Fluids* **13**, 2634

Launder, B., Reece, G., and Rodi, W.: 1975, *J. Fluid Mech.* **68(3)**, 537

Launder, B. and Sharma, B.: 1974, *Letters in Heat an Mass Transfer* **1(2)**, 131

Launder, B. and Shima, N.: 1989, *AIAA J.* **27**, 1319

Lee, M., Kim, J., and Moin, P.: 1990, *J. Fluid Mech.* **216**, 561

Lee, M. and Reynolds, W.: 1985, *Numerical Experiments on the Structure of Homogeneous Turbulence*, Technical Report TF-24, Thermosciences Division, Department of Mechanical Engineering, Stanford University

Matsumoto, A., Nagano, Y., and Tsuji, T.: 1991, in 5^{th} *Symposium on Computational Fluid Dynamics*, pp 361–64, Tokyo

Pope, S.: 2000, *Turbulent flows*, Cambridge University Press

Rogers, M. and Moin, P.: 1987, *J. Fluid Mech.* **176**, 33

Scotti, A. and Piomelli, U.: 2001, *Phys. Fluids* **13(5)**, 1367

Shima, N.: 1998, *Int. J. Heat and Fluid Flow* **19**, 549

Speziale, C., Sarkar, S., and Gatski, T.: 1991, *J. Fluid Mech.* **227**, 245

Yu, D. and Girimaji, S.: 2006, *J. Fluid Mech.* **566**, 117